frontiers in Molecular Neuroscience

ORIGINAL RESEARCH
published: 13 May 2021
doi: 10.3389/fnmol.2021.631833

# Dephosphorylation Passivates the Seeding Activity of Oligomeric Tau Derived From Alzheimer's Brain

*Ruozhen Wu[1,2†], Longfei Li[1,2†], Ruirui Shi[1,2], Yan Zhou[1,2], Nana Jin[1], Jianlan Gu[1,2], Yunn Chyn Tung[2], Fei Liu[2]* and Dandan Chu[1]**

[1] NMPA Key Laboratory for Research and Evaluation of Tissue Engineering Technology Products, Key Laboratory of Neuroregeneration of Jiangsu and Ministry of Education, Co-innovation Center of Neuroregeneration, Nantong University, Nantong, China, [2] Department of Neurochemistry, Inge Grundke-Iqbal Research Floor, New York State Institute for Basic Research in Developmental Disabilities, Staten Island, NY, United States

Accumulation of intracellular neurofibrillary tangles (NFTs), which are constituted of abnormally phosphorylated tau, is one of the neuropathological hallmarks of Alzheimer's disease (AD). The oligomeric aggregates of tau in AD brain (AD O-tau) are believed to trigger NFT spreading by seeding normal tau aggregation as toxic seeds, in a prion-like fashion. Here, we revealed the features of AD O-tau by Western blots using antibodies against various epitopes and determined the effect of dephosphorylation on the seeding activity of AD O-tau by capture and seeded aggregation assays. We found that N-terminal truncated and C-terminal hyperphosphorylated tau species were enriched in AD O-tau. Dephosphorylation of AD O-tau by alkaline phosphatase diminished its activity in capturing tau *in vitro* and in inducing insoluble aggregates in cultured cells. Our results suggested that dephosphorylation passivated the seeding activity of AD O-tau. Inhibition of phosphorylation may be a potent strategy to prevent the spreading of tau patho3logy.

**Keywords: Alzheimer's disease, neurofibrillary tangles, oligomeric tau derived from AD brain, dephosphorylation, seeding activity**

OPEN ACCESS

***Edited by:***
*Javier Egea,*
*Princess University Hospital, Spain*

***Reviewed by:***
*Caroline Smet-Nocca,*
*Université de Lille, France*
*Urmi Sengupta,*
*University of Texas Medical Branch at Galveston, United States*
*Marcos Jair Guerrero-Munoz,*
*Autonomous University of Nuevo León, Mexico*

***Correspondence:**
*Fei Liu*
*feiliu63@hotmail.com*
*Dandan Chu*
*chudd@ntu.edu.cn*

*† These authors have contributed equally to this work*

***Received:** 21 November 2020*
***Accepted:** 26 March 2021*
***Published:** 13 May 2021*

***Citation:***
*Wu R, Li L, Shi R, Zhou Y, Jin N, Gu J, Tung YC, Liu F and Chu D (2021) Dephosphorylation Passivates the Seeding Activity of Oligomeric Tau Derived From Alzheimer's Brain. Front. Mol. Neurosci. 14:631833. doi: 10.3389/fnmol.2021.631833*

## INTRODUCTION

The microtubule-associated protein tau is a highly water-soluble and basic protein. Normal tau stabilizes microtubules *in vitro* by binding to the interface between tubulin heterodimers with its microtubule-binding repeats (Kadavath et al., 2015). As a phosphoprotein, tau contains more than 80 residues that can potentially be phosphorylated, and at least 18 of these sites are abnormally hyperphosphorylated in the brains of Alzheimer's patients (Chu and Liu, 2018; Iqbal et al., 2018). Hyperphosphorylated tau detaches from microtubules, resulting in microtubule loss in neurons (Austin et al., 2017). Accumulation of intracellular neurofibrillary tangles (NFTs), which mainly consist of hyperphosphorylated and truncated tau, is correlated directly with the degree of cognitive decline in AD patients and is considered as one of the predominant hallmarks of AD.

The NFT pathology in AD brains initiates in the locus coeruleus and transentorhinal area, and sequentially progresses to the limbic system and further to the isocortex, as described in the Braak stages (Braak and Braak, 1991). Intrahippocampal injection of tau aggregates isolated from AD patients or produced *in vitro* successfully induced tau hyperphosphorylation and NFT formation at the injection sites and anatomically related regions in rodent brains, showing a similar stereotypical propagation of tau pathology as observed in AD brain (Clavaguera et al., 2009; Boluda et al., 2015;

Takeda et al., 2015; Hu et al., 2016; Miao et al., 2019). Emerging evidence suggests that the prion-like seeding activity of pathological tau in AD brain is crucial for its propagation. Due to the induction of molecules with strong negative charges (such as heparin and RNA) or even proteins, the inert tau monomer could switch its conformation to form β-sheet structures that are prone to oligomerization (Goedert et al., 1996; Mudher et al., 2017; Wischik et al., 2018). The oligomeric tau aggregates, acting like "seeds," capture normal tau proteins and template their conformational change in a prion-like mechanism, and eventually assembles the paired helical filaments (PHFs) and NFTs in neurons (von Bergen et al., 2005; Lasagna-Reeves et al., 2012b). Oligomeric tau isolated from Alzheimer's brain (AD O-tau) has been reported to capture tau protein *in vitro*, seed tau aggregation in cultured cells, and induce the propagation of tau pathology in rodent brains (Lasagna-Reeves et al., 2012a; Hu et al., 2016; Li et al., 2019).

Our previous studies showed that high-molecular-weight oligomers of tau (HMW-tau) were specifically accumulated in the brain of AD patients. HMW-tau lacked the N-terminal portion and was hyperphosphorylated at multiple sites including Ser199, Ser202, Thr205, Thr212, Ser214, Thr217, Ser262, Ser396, Ser404, and Ser422 (Zhou et al., 2018; Li et al., 2019). According to the reported cleavage sites on human tau in AD brain (Wang et al., 2010; Zhang et al., 2014), we deleted the first 50, 150 or 230 amino acids (a.a.) and the last 20 or 50 a.a. of the longest human tau isoform tau441, examined the pathological activities of each truncated isoforms, and found that deletion of the first 150 and the last 50 a.a. of tau enhanced its site-specific phosphorylation, self-aggregation, and captured and seeded aggregation by AD O-Tau (Gu et al., 2020).

Dephosphorylation of AD hyperphosphorylated tau with protein phosphatases such as protein phosphatase 2A (PP2A) restored the microtubule polymerization activity of tau (Wang et al., 1996). Dephosphorylation with alkaline phosphatase (AP) or PP2A diminished the ability of hyperphosphorylated tau in inducing aggregation, prevented tangle formation *in vitro* (Alonso et al., 1996), and reduced the number of NFTs in mouse brain (Hu et al., 2016). However, the mechanism that dephosphorylation inhibits the prion-like activity of toxic tau seeds remains unclear.

In the present study, we isolated oligomeric tau from AD brains and analyzed AD O-tau by Western blots using antibodies against different epitopes of tau protein. We found that AD O-tau was mainly N-terminal truncated and C-terminal hyperphosphorylated. AP treatment successfully reduced the phosphorylation of AD O-tau. Tau capture assay revealed that compared with AD O-tau, the ability of dephosphorylated AD O-tau (Dp-AD O-tau) to capture free tau is decreased. Immunofluorescence showed that Dp-AD O-tau templated less aggregates formation in HeLa cells. Seeded tau aggregation assay in HEK-293FT cells revealed that Dp-AD O-tau induced less accumulation of total and phosphorylated tau in the insoluble fractions from cell lysates. Our results suggested that dephosphorylation could be an effective way to passivate the prion-like seeding activity of AD O-tau.

# MATERIALS AND METHODS

## Human Brain Samples

Frozen frontal cortices from autopsied and histopathologically confirmed AD (80 years old, female, 2.9 h post mortem interval, Harvard Brain Tissue Resource Center McLean Hospital) and age-matched normal human (84 years old, female, 4.25 h post mortem interval, De Nederlandse Hersenbank) brains were obtained without identification of donors. Brain samples were frozen at −80°C until analysis. The use of postmortem human brain tissue was in accordance with the National Institutes of Health Guidelines and was exempted by the Institutional Review Board of New York State Institute for Basic Research in Developmental Disabilities because "the research does not involve intervention or interaction with the individuals," nor "is the information individually identifiable."

## Preparation of AD O-Tau, Dephosphorylated-AD O-Tau (Dp-AD O-Tau), and Heat-Stable Tau (HS-Tau)

AD O-tau was isolated from frozen autopsy cerebral cortex of AD patient as described (Kopke et al., 1993). Briefly, the brain tissue was homogenized in ninefold volume of ice-cold lysis buffer containing 20 mM Tris-HCl, pH 8.0, 0.32 M sucrose, 10 mM β-mercaptoethanol, 10 mM glycerophosphate, 5 mM $MgSO_4$, 50 mM NaF, 1 mM EDTA, 1 mM $Na_3VO_4$, 1 mM 4-(2-aminoethyl) benzenesulfonyl fluoride hydrochloride (AEBSF), and 10 μg/ml each of aprotinin, leupeptin, and pepstatin. The homogenate was centrifuged at 27,000 × *g* for 30 min at 4°C. The supernatant was aspirated and further centrifuged at 235,000 × *g* for 45 min at 4°C. The resulting pellet rich in AD O-tau was collected, washed twice, and resuspended in saline. AD O-Tau was stored at −80°C and probe-sonicated for 2 min (0.5 s on, 3 s off) at 20% power before use.

The supernatant was saved and NaCl was added to a final concentration of 0.75 M. The remaining aggregated tau in the supernatant was removed by boiling for 5 min. After cooling, the samples were centrifuged at 25,000 × *g* for 30 min. The supernatant was collected, dialyzed against 10 mM Tris-HCl, pH 7.6, and concentrated by five times to obtain HS-tau.

Dp-AD O-tau was obtained by incubating AD O-tau (4 mg/ml protein) with 196 U/ml AP in the reaction buffer (100 mM Tris-HCl, pH 8.0, 1 mM phenylmethylsulfonyl fluoride, 2 μg/ml aprotinin, 2 μg/ml pepstatin, and 5 μg/ml leupeptin) at 37°C for 5 h. Dephosphorylated products were analyzed by Western blots developed with Tau-1 antibody to show dephosphorylation efficacy.

## Dephosphorylation of AD O-Tau on Nitrocellulose Membrane

Various amounts of AD O-tau were spotted on a nitrocellulose membrane (Schleicher and Schuell, Keene, NH, United States) at 5 μl/grid of 7 × 7 mm. The membrane was incubated at 37°C for 1 h to allow protein binding to the membrane. Proteins on the membrane were dephosphorylated as described previously (Kopke et al., 1993) with slight modification. The membrane was

wet by TBS and incubated with 196 U/ml AP in the reaction buffer as described above at 37°C for 5 h. After blocking with 5% milk in TBS (50 mM Tris-HCl, pH 7.4, 150 mM NaCl) for 30 min, membrane was then developed with specific antibodies or subjected to tau capture assay.

## Western Blots and Dot Blots

Brain homogenates were prepared in 10% in ice-cold lysis buffer consisting of 50 mM Tris-HCl, pH 7.4, 8.5% sucrose, 2.0 mM EDTA, 10 mM β-mercaptoethanol, 1 mM $Na_3VO_4$, 50 mM NaF, 1 mM AEBSF, and 10 μg/ml each of aprotinin, leupeptin, and pepstatin. The homogenates were diluted in 2 × Laemmli sample buffer (250 mM Tris-HCl, pH 6.8, 20% glycerol, 20% β-mercaptoethanol, 4% SDS and 0.008% bromophenol blue), followed by boiling for 10 min. Protein concentration of each sample was measured by the Pierce™ 660 nm Protein Assay kit (Thermo Fisher Scientific, Waltham, MA, United States). Same amounts of protein in brain homogenate were subjected to sodium dodecyl sulfate-polyacrylamide gel electrophoresis (SDS-PAGE) and electro-transferred to a polyvinylidene difluoride (PVDF) membrane.

For dot blots, the cells were lysed with RIPA (radio immunoprecipitation assay) buffer (50 mM Tris-HCl, pH 7.4, 150 mM NaCl, 1% Non-idet P-40, 0.5% sodium deoxycholate, 0.1% SDS, 50 mM NaF, 1 mM $Na_3VO_4$, 1 mM AEBSF, 5 mM benzamidine, and 10 μg/ml each of aprotinin, leupeptin, and pepstatin) and the protein concentration was determined. Different amounts of protein were spotted on a nitrocellulose membrane (Schleicher and Schuell, Keene, NH, United States) at 5 μl/grid of 7 × 7 mm. The blot was incubated at 37°C for 1 h to allow protein binding to the membrane.

The PVDF or nitrocellulose membrane was blocked with 5% skim milk in TBS buffer (50 mM Tris-HCl, pH 7.4, and 150 mM NaCl) for 30 min and was subsequently incubated overnight with specific primary antibodies (**Table 1**) at room temperature. After washing three times with TBST (TBS containing 0.05% Tween-20), the membrane was incubated with horseradish peroxidase (HRP)-conjugated secondary antibody (1:4,000, Jackson ImmunoResearch, West Grove, PA, United States) at room temperature for 2 h, washed with TBST, incubated with enhanced chemiluminescence (ECL) kit (Thermo Fisher Scientific, Rockford, IL, United States), and exposed to X-ray films (Denville Science, Holliston, MA, United States). The intensity of bands on Western blots and dot blots was quantified by Multi Gauge software (Fujifilm, Mito, Tokyo, Japan).

## Cell Culture and Plasmids

HEK-293FT and HeLa cell lines were maintained in Dulbecco's modified Eagle's medium (DMEM) supplemented with 10% fetal bovine serum (Thermo Fisher Scientific, Waltham, MA, United States) at 37°C in a humidified atmosphere of 5% $CO_2$/95% air.

pCI/HA (hemagglutinin)-tau$_{1-441}$ and pCI/HA-tau$_{151-391}$ were generated as previously described (Gu et al., 2020). The DNA sequence of the plasmids was confirmed by Sanger sequencing. PCI-neo plasmid was used as a negative control. pCI/HA-tau$_{1-441}$ or pCI/HA-tau$_{151-391}$ was transfected into HEK-293FT or HeLa cells by FuGENE® HD Transfection Reagent (Promega, Madison, WI, United States) following the manufacturer's instructions.

## Seeded Tau Aggregation in Cultured Cells

HEK-293FT cells were transfected with pCI/HA-tau$_{1-441}$ or pCI/HA-tau$_{151-391}$. AD O-Tau or Dp-AD O-tau was sonicated

**TABLE 1 |** Primary antibodies used in this study.

| Antibody | Type | Specificity | Working dilution | Species | Source (catalog number) |
|---|---|---|---|---|---|
| 113e | Polyclonal | Pan-tau (a.a. 19–32) | 1:1,000 | Rabbit | In-house |
| 43D | Monoclonal | Pan-tau (a.a. 6–18) | 1:1,000 | Mouse | BioLegend (816601) |
| 77G7 | Monoclonal | Pan tau (a.a. 244–368) | 1:1,000 | Mouse | BioLegend (816701) |
| 92e | Polyclonal | Pan-tau | 1:1,000 | Rabbit | In-house |
| Anti-HA | Polyclonal | HA | 1:2,000 | Rabbit | Sigma (H6908) |
| Anti-HA | Monoclonal | HA | 1:30,000 | Mouse | Sigma (H9658) |
| Anti-pT181 | Monoclonal | Phospho-tau (T181) | 1:500 | Mouse | Invitrogen (MN1050) |
| Anti-pS199 | Polyclonal | Phospho-tau (S199) | 1:1,000 | Rabbit | Invitrogen (44-734G) |
| Anti-pT212 | Polyclonal | Phospho-tau (T212) | 1:500 | Rabbit | Invitrogen (44-740G) |
| Anti-pS214 | Polyclonal | Phospho-tau (T214) | 1:1,000 | Rabbit | Invitrogen (44-742G) |
| Anti-pT217 | Polyclonal | Phospho-tau (T217) | 1:500 | Rabbit | Invitrogen (44-744) |
| Anti-pS262 | Polyclonal | Phospho-tau (S262) | 1:500 | Rabbit | Invitrogen (44-750G) |
| Anti-pS422 | Polyclonal | Phospho-tau (S422) | 1:500 | Rabbit | Invitrogen (44-764G) |
| HT7 | Monoclonal | Pan-tau (a.a. 159–163) | 1:1,000 | Mouse | Invitrogen (MN1000) |
| PHF-1 | Monoclonal | Phospho-tau (S396/404) | 1:500 | Mouse | Dr. Peter Davies |
| R134d | Polyclonal | Pan-tau | 1:10,000 | Rabbit | In-house |
| Tau-1 | Monoclonal | Unphosphorylated-tau (a.a. 195,198,199, and 202) | 1:500 | Mouse | Dr. Lester I. Binder |
| Tau46 | Monoclonal | Pan tau (a.a. 404–421) | 1:1,000 | Mouse | Invitrogen (13-6400) |
| TAU-5 | Monoclonal | Pan-tau (a.a. 210–230) | 1:1,000 | Mouse | Invitrogen (AHB0042) |
| GAPDH | Monoclonal | GAPDH | 1:1,000 | Mouse | Santa Cruz (sc-47724) |

at 20% power for 2 min (0.5 s on, 3 s off) before use. Six hours after transfection, AD O-Tau or Dp-AD O-tau was mixed with 3% Lipofectamine 2000 (Invitrogen, Carlsbad, CA, United States) in Opti-MEM (Thermo Fisher Scientific, Waltham, MA, United States) for 20 min at room temperature and then added into the cell culture at a final concentration of 6.6 μg/ml. Forty-eight hours after transfection, the cells were harvested and analyzed for tau aggregation by Western blots or immunofluorescence.

To examine the accumulation of insoluble tau, the cells were lysed in RIPA buffer for 20 min on ice and centrifuged at 130,000 × *g* for 45 min. The supernatants were collected as RIPA-soluble fraction and diluted in 4 × Laemmli sample buffer. The resulting pellets containing the insoluble fraction were washed twice with RIPA buffer and resuspended in 1 × Laemmli buffer by sonicating at 80% power for 8 min (5 s on, 20 s off) with sonicator equipped with cup horn (Thermo Fisher Scientific, Waltham, MA, United States). The samples were boiled for 5 min. Levels of RIPA-insoluble and -soluble tau were determined by Western blots developed with anti-HA antibody (**Table 1**). Levels of phosphorylated tau at each specific site were analyzed by Western blots developed with site-specific and phosphorylation-dependent tau antibodies.

## Immunofluorescence

HeLa cells were transfected with pCI/HA-tau$_{1-441}$ or pCI/HA-tau$_{151-391}$ by FuGENE® HD and treated with 6.6 μg/ml AD O-tau or Dp-AD O-tau as described above. The cells were harvested, fixed for 15 min with 4% paraformaldehyde in phosphate-buffered saline (PBS), and treated with 0.3% Triton in PBS for 15 min. After blocking with 5% newborn goat serum, 0.05% Tween-20, and 0.1% Triton X-100 in PBS for 30 min, the cells were incubated with 77G7 (1:500) or anti-HA (1:1,000) antibody in the blocking solution overnight at 4°C. After washing three times with PBS, the cells were incubated with Alexa Fluor 555-conjugated or 488-conjugated IgG (1:1,000, Thermo Fisher Scientific, Waltham, MA, United States) for 2 h and TO-PRO-3 (5 mg/ml, Thermo Fisher Scientific, Waltham, MA, United States) for 15 min at room temperature. After washing with PBS, the cells were mounted using ProLong™ Gold Antifade Mountant (Thermo Fisher Scientific, Waltham, MA, United States). The images were captured with a Nikon EZ-C1 confocal microscope (Nikon Instruments, Melville, NY, United States).

The number of HA-tau$_{151-391}$-expressing cells and the number of cells with tau aggregates were counted under the microscope. The percentage of cells with tau aggregates was calculated by dividing the number of cells with aggregates by the total number of HA-tau$_{151-391}$-expressing cells on each slide.

## Tau Capture Assay

Tau capture assay was carried out as described (Kremer et al., 1988; Alonso et al., 1994; Li et al., 2019). HEK-293FT cells overexpressing pCI/HA-tau$_{151-391}$ were lysed in PBS containing 50 mM NaF, 1 mM $Na_3VO_4$, 1 mM AEBSF, 5 mM benzamidine, and 10 μg/ml each of aprotinin, leuprotinin, and pepstatin. The cell lysate was sonicated at 20% power for 2 min (0.5 s on, 3 s off) and centrifuged at 10,000 × *g* for 10 min to extract the supernatant containing HA-tau$_{151-391}$. Different amounts of AD O-tau or HS-tau were spotted on the nitrocellulose membrane and dried at 37°C for 1 h. The membrane was then blocked with 5% skim milk in TBS for 1 h, and incubated overnight with the cell extract containing HA-tau$_{151-391}$. After washing three times with TBST, the membrane was examined by anti-HA antibody using dot blot method.

## Statistical Analysis

Data were presented as mean ± standard deviation (SD). The statistical significance was analyzed by one-way analysis of variance (ANOVA) followed by Tukey's *post hoc* test for multiple comparisons using GraphPad Prism 8 (GraphPad Software Inc., San Diego, CA, United States). $P < 0.05$ was considered statistically significant.

# RESULTS

## AD O-Tau Is Mainly N-Terminal Truncated and C-Terminal Hyperphosphorylated

Truncation and hyperphosphorylation of tau are commonly found in AD brains (Zhou et al., 2018; Li et al., 2019). Brain-derived tau oligomers from the individuals with AD and related tauopathies can capture normal tau and trigger the propagation of tau pathology as cytotoxic seeds (Hu et al., 2016; Chu and Liu, 2018). To determine whether oligomeric tau from AD brain is also hyperphosphorylated and/or truncated, AD O-tau was analyzed by Western blots developed with antibodies raised against specific epitopes of tau (**Figure 1A** and **Table 1**). R134d, a polyclonal antibody raised against the longest human tau isoform, tau441 (Tatebayashi et al., 1999), detected smear bands in AD O-tau and AD brain lysate but not in control brain lysates, confirming the truncation and SDS- and β-mercaptoethanol-resistant high-molecular weight of AD O-tau (**Figure 1B**). Monoclonal antibodies 43D and HT7, which recognize the N-terminal 6–18 a.a. and 159–163 a.a. of tau441, respectively, detected tau bands in both control and AD brain lysates, but not in AD O-tau. Similar results were found when using the polyclonal antibody 113e (Li et al., 2019) that recognizes 19–32 a.a. of tau, indicating that AD O-tau was mostly N-terminal truncated (**Figure 1B**). 77G7 (244–368 a.a.) and Tau5 (210–230 a.a.) that target the epitopes in or close to the microtubule binding repeats of tau both showed stronger affinity to AD O-tau than to AD or control brain lysates. The level of tau detected by Tau46 (404–421 a.a.) was decreased in AD O-tau, implying that AD O-tau could be partially C-terminal truncated. These results suggested that truncated tau species were accumulated in AD O-tau.

Tau is abnormally hyperphosphorylated in AD brain (Zhou et al., 2018). Therefore, we used a series of phosphorylation site-specific antibodies of tau to examine the phosphorylation pattern of AD O-tau (**Figure 1C**). Phosphorylation of all the epitopes tested, pS199, pT217, pS262, pS396/404, and pS422, were increased in AD compared to control lysate, consistent with previous reports (Zhou et al., 2018). However, the changes of

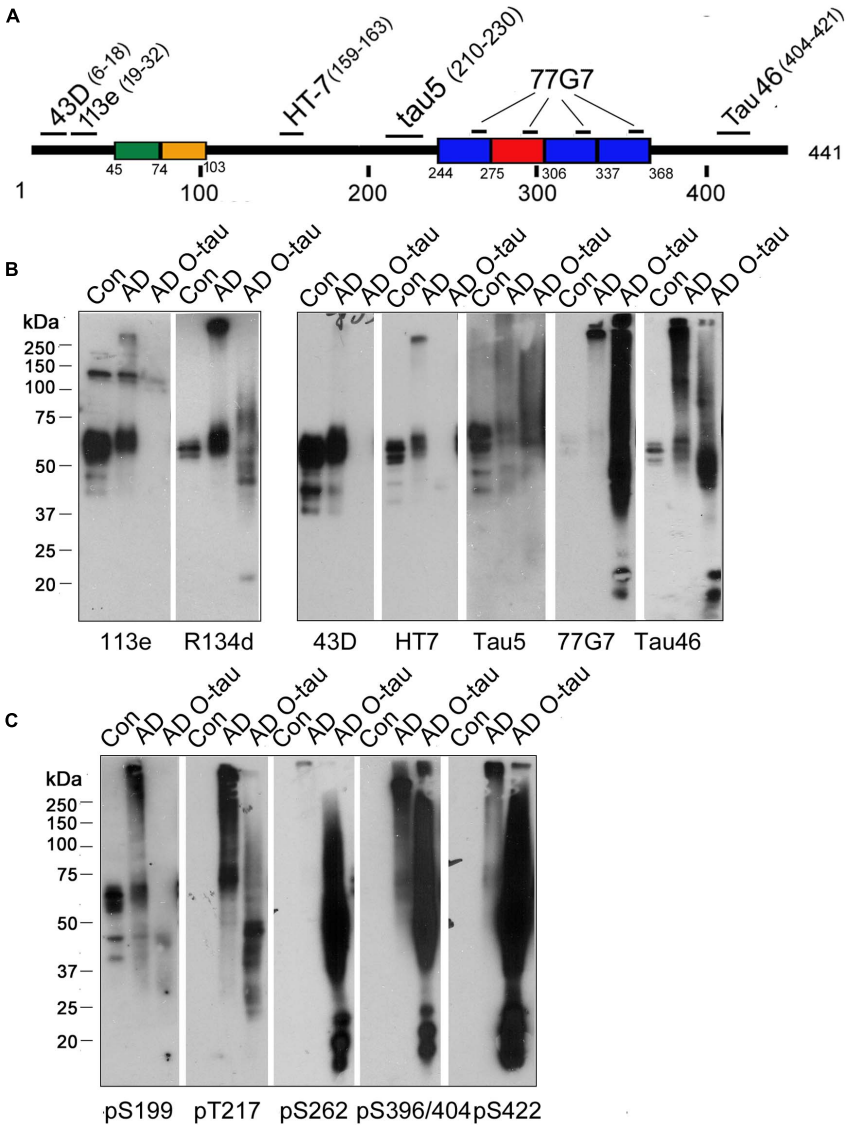


**FIGURE 1 |** AD O-tau was N-terminal truncated C-terminal hyperphosphorylated. **(A)** The diagram of the longest human tau isoform ($tau_{441}$) showing the epitopes recognized by various pan-tau antibodies used in this study. **(B,C)** AD O-tau and the homogenates from AD and control human brains were analyzed by Western blots developed with polyclonal or monoclonal pan-tau antibodies **(B)** and site-specific and phosphorylation-dependent tau antibodies **(C)**.

site-specific phosphorylation in AD O-tau were not the same as that in AD lysate. In AD O-tau, pS199 phosphorylation was distinctly eliminated, which might be because of tau cleavage at the N-terminus. pT217 showed comparable phosphorylation levels in AD O-tau and AD lysate. Phosphorylation of pS262, pS396/404, and pS422 was dramatically elevated in AD O-tau than in AD and control lysate. The site-selective phosphorylation of AD O-tau implied that C-terminal hyperphosphorylated tau species were prone to aggregate in AD O-tau.

## Dephosphorylation Inhibits the Ability of AD O-Tau to Capture $Tau_{151-391}$

Recently, we constructed 11 truncated forms of full-length tau and analyzed the pathological activities of them (Gu et al., 2020). We found that deletion of the first 150 or 230 a.a. and the last 50 a.a. of tau enhanced its site-specific phosphorylation and seeded aggregation by AD O-Tau. Among these truncated proteins, $tau_{151-391}$ exhibited the highest pathological activities but did not show significant difference in cytotoxicity compared with full-length tau ($tau_{1-441}$) (Gu et al., 2020). In the present study, HeLa cells were transfected with HA-$tau_{1-441}$ or HA-$tau_{151-391}$. Six hours later, the cells were treated with AD O-tau for 42 h and then subjected to immunofluorescence. The immunofluorescence staining with 77G7 antibodies revealed that both HA-$tau_{1-441}$ and HA-$tau_{151-391}$ were expressed in HeLa cells. AD O-tau induced remarkable aggregates in the cytoplasm and nucleus of HA-$tau_{151-391}$-expressing cells, but only diffusion distribution of tau in HA-$tau_{1-441}$-transfected cells (**Figure 2A**).

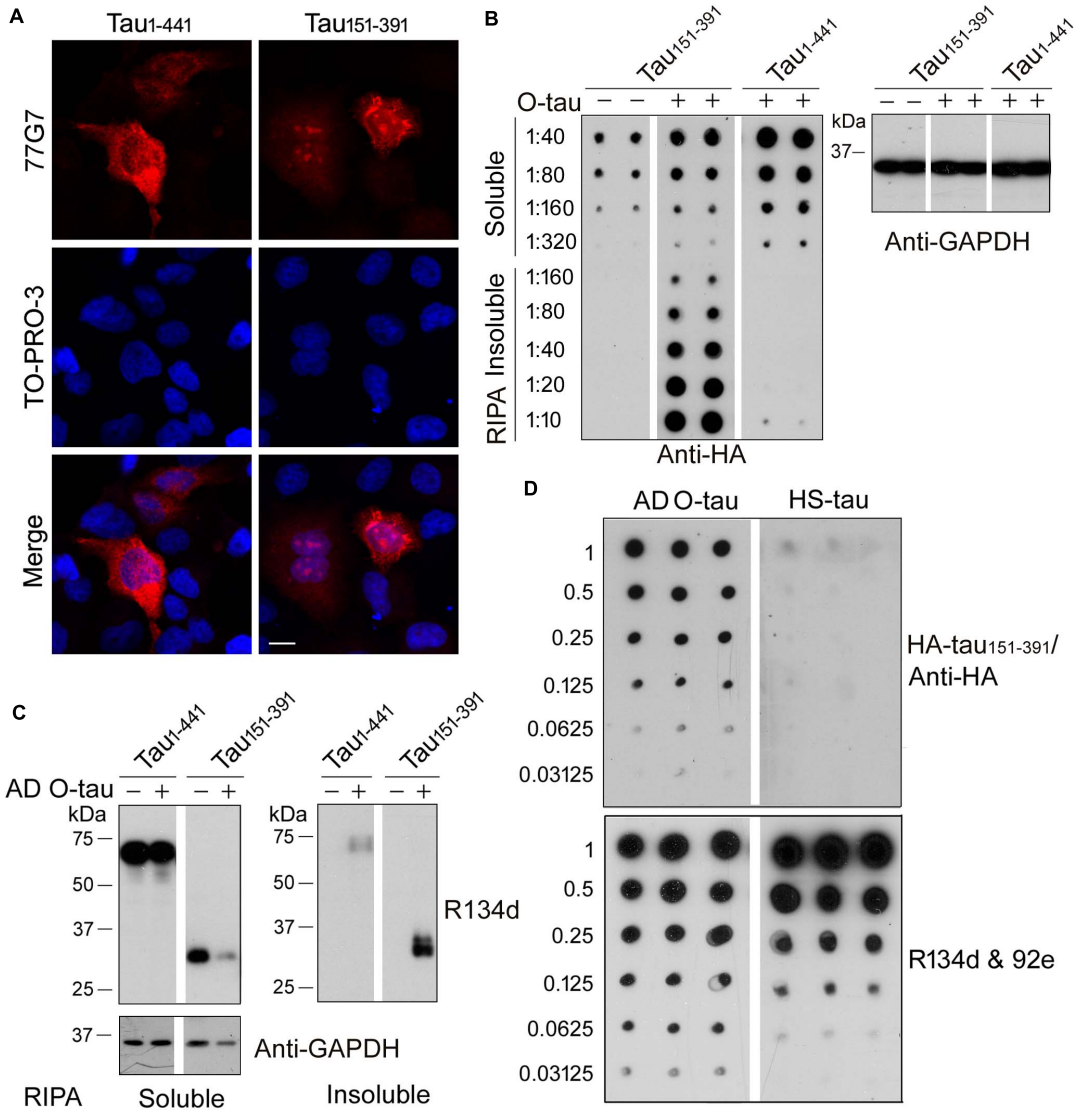


**FIGURE 2 |** AD O-tau captured HA-tau$_{151-391}$ *in vitro* and seeded its aggregation in cultured cells. **(A)** HeLa cells were transfected with pCI/HA-tau$_{1-441}$ or pCI/HA-tau$_{151-391}$, treated with AD O-tau for 42 h and immunostained with tau antibody 77G7 (red). Cell nuclei were labeled by TO-PRO-3 (blue). Bar, 10 μm. **(B,C)** HEK-293FT cells were transfected with pCI/HA-tau$_{1-441}$ or pCI/HA-tau$_{151-391}$, treated with AD O-tau for 42 h and lysed with RIPA buffer. RIPA buffer-soluble and -insoluble fractions were separated by centrifuging at 130,000 × *g* for 45 min. Dilution series of RIPA-soluble or -insoluble samples were applied on nitrocellulose membranes and detected with anti-HA antibody. Corresponding cell lysates from parallel experiment were analyzed by Western blot developed with anti-GAPDH **(B)**. RIPA-soluble or -insoluble samples were analyzed by Western blots developed with anti-tau (R134d and 92e) and anti-GAPDH antibodies **(C)**. **(D)** A series of concentration gradients of AD O-tau or heat-stable tau (HS-tau) were applied on nitrocellulose membranes. The membrane was incubated with HEK-293FT cell lysate expressing HA-tau$_{151-391}$. HA-tau$_{151-391}$ captured by AD O-tau or HS-tau was detected with anti-HA antibody. The total amount of AD O-tau or HS-tau on the membrane was determined by the mixture of pan-tau antibodies, R134d and 92e.

For biochemical analyses, HEK-293FT cells were transfected with HA-tau$_{1-441}$ or HA-tau$_{151-391}$, treated with AD O-tau for 42 h and then lysed with RIPA buffer and centrifuged at 130,000 × *g* for 45 min to separate RIPA-insoluble pellets and RIPA-soluble supernatants. Serial dilutions of the RIPA-soluble or -insoluble samples were spotted on nitrocellulose membranes and subjected to dot blots using anti-HA antibody (**Figure 2B**). The results showed higher level of RIPA-soluble tau in HEK-293FT/HA-tau$_{1-441}$ cells than in HEK-293FT/HA-tau$_{151-391}$ cells. O-tau treatment induced intensive insoluble aggregates of HA-tau$_{151-391}$, but not that of HA-tau$_{1-441}$. Next, RIPA-soluble or -insoluble fraction from HA-tau$_{1-441}$- or HA-tau$_{151-391}$-expressing cells treated with or without AD O-tau were examined by Western blots developed with tau antibodies (**Figure 2C**). AD O-tau induced dramatic accumulation of tau$_{151-391}$ in RIPA-insoluble fraction, whereas less tau$_{151-391}$ in RIPA-soluble fraction, compared with tau$_{1-441}$. These results further support that tau$_{151-391}$ could be more susceptible to AD O-tau seeded

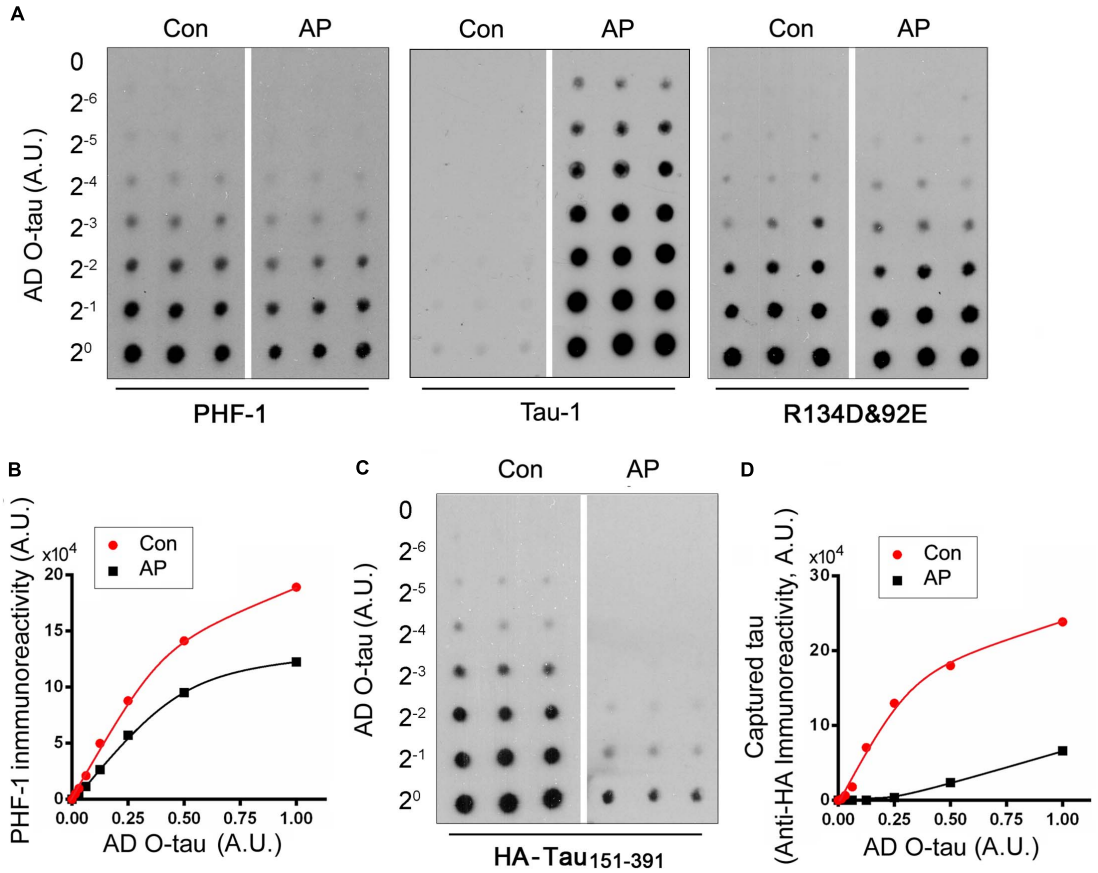


**FIGURE 3 |** Dephosphorylation of AD O-tau inhibited its ability to capture HA-tau$_{151-391}$ *in vitro*. **(A,B)** A series of concentration gradients of AD O-tau were applied onto nitrocellulose membranes. One set of membranes were treated with alkaline phosphatase (AP) to dephosphorylate AD O-tau. The control membranes were incubated with only the reaction buffer. The membranes were then developed with PHF-1 (anti-pS396/404 tau) or a mixture of R134d and 92e (pan-tau) to analyze the phosphorylation and total levels of AD O-tau, respectively **(A)**. The relative levels of PHF-1 immunoreactivity were plotted against the amounts of AD O-tau or Dp-AD O-tau **(B)**. **(C,D)** Control or AP-treated membranes were incubated with HEK-293FT cell lysate expressing HA-tau$_{151-391}$ and developed with anti-HA antibody to measure the levels of HA-tau$_{151-391}$ captured by AD O-tau or Dp-AD O-tau **(C)**. Anti-HA immunoreactivity was plotted against the amounts of AD O-tau and Dp-AD O-tau **(D)**.

aggregation. Thus, HA-tau$_{151-391}$, instead of HA-tau$_{1-441}$, was used in the following analyses for tau seeding activity.

Normal tau is heat-stable (Weingarten et al., 1975). Heat treatment is commonly used to remove tau aggregates from the soluble fraction of brain lysate (Planel et al., 2007; Miao et al., 2019). Various amounts of AD O-tau or heat-stable tau (HS-tau) were dotted on nitrocellulose membranes, which were further incubated with cell lysate containing HA-tau$_{151-391}$ to allow the capture of HA-tau$_{151-391}$ by AD O-tau or HS-tau. Captured HA-tau$_{151-391}$ was detected by anti-HA antibody (**Figure 2D**). The results indicated that AD O-tau, but not HS-tau, captured HA-tau$_{151-391}$ (**Figure 2D**).

To determine the role of phosphorylation in modulating the capture ability of AD O-tau, we applied various amount of AD O-tau onto nitrocellulose membranes parallelly. One set of membranes was treated with AP to dephosphorylate AD O-tau on it. The control membranes were treated with the reaction buffer parallelly. Dephosphorylation of AD O-tau by AP was identified by reduced PHF-1 (recognizing phosphorylated tau at Ser396/404) and enhanced Tau-1 (recognizing tau unphosphorylated Ser195/198/199/202) immunoreactivity (**Figures 3A,B**). Similar R134d (Tatebayashi et al., 1999) and 92e (Grundke-Iqbal et al., 1988) immunoreactivity indicated that AP treatment did not affect total tau levels on the membrane (**Figure 3A**). The control and AP-treated membranes were further incubated with cell lysate containing HA-tau$_{151-391}$ to allow the binding of HA-tau$_{151-391}$ to AD O-tau. Captured HA-tau$_{151-391}$ developed with anti-HA was markedly decreased in AP-treated membrane, suggesting that dephosphorylation of AD O-tau inhibited its ability to capture tau (**Figures 3C,D**).

## Dephosphorylation Inhibits AD O-Tau-Induced Aggregation of Tau$_{151-391}$

To assess the ability of dephosphorylated AD O-tau (Dp-AD O-tau) in triggering tau aggregation, we used AP to dephosphorylate AD O-tau and added Dp-AD O-tau into

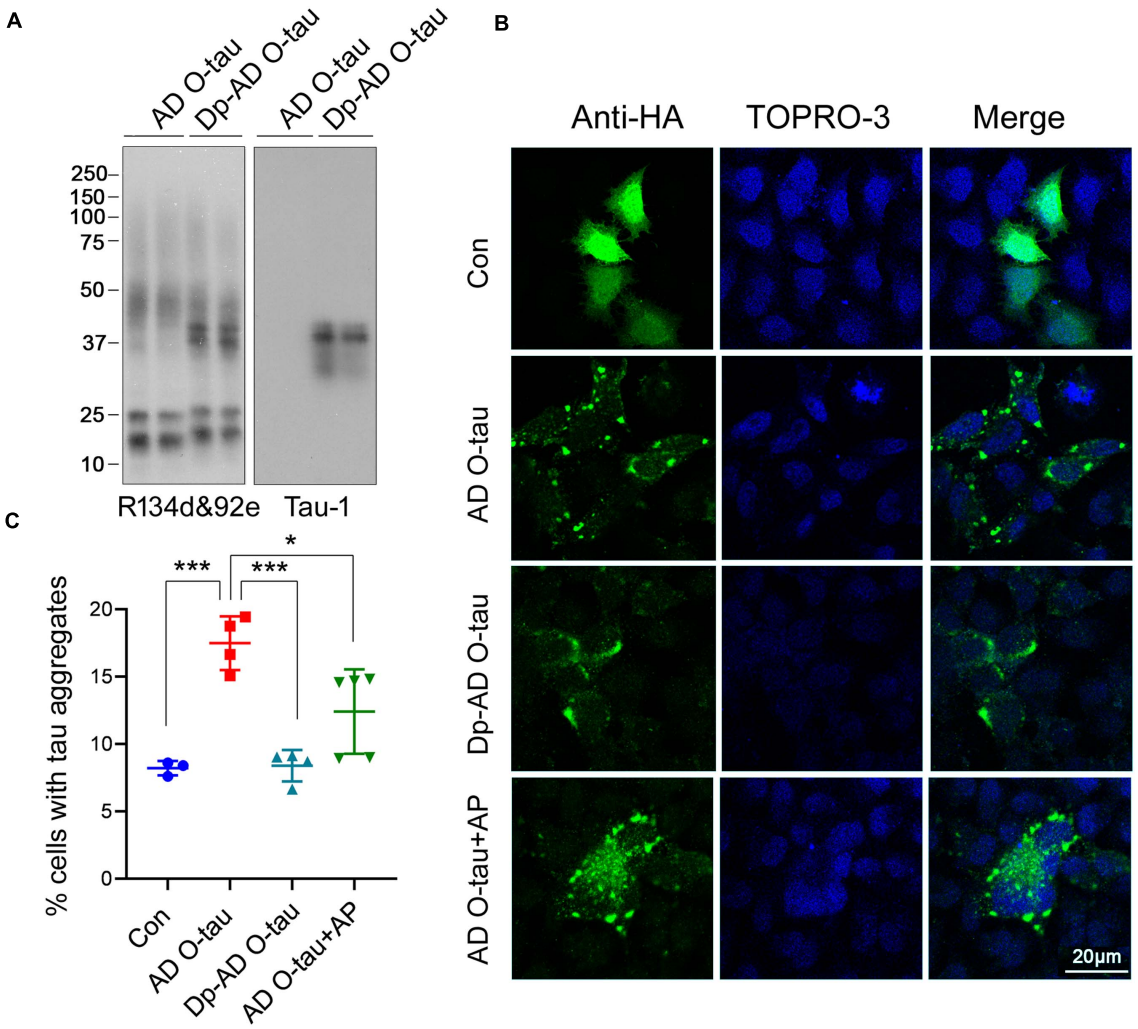


**FIGURE 4 |** Dephosphorylation of AD O-tau inhibited its ability to seed tau aggregation in HeLa cells. **(A)** AD O-tau and Dp-AD O-tau were analyzed by Western blots developed with a mixture of R134d and 92e (pan-tau) or Tau-1 (unphosphorylated tau). **(B,C)** HeLa cells were transfected with pCI/HA-tau$_{151-391}$, treated with AD O-tau, Dp-AD-O-tau, or AD O-tau and AP for 42 h, and immunostained with anti-HA antibody (**B**, green). Cell nuclei were labeled by TO-PRO-3 (**B**, blue). Bar, 20 μm. The number of HA-tau$_{151-391}$-expressing cells and the number of cells with tau aggregates were counted **(C)**. The experiment was performed in triplicate wells and eight fields were photographed from each well of each group. Percentage of cells with aggregated tau was determined. Each experiment was repeated at least twice. *$P < 0.05$. ***$P < 0.001$.

HeLa cells expressing HA-tau$_{151-391}$ to investigate the formation of aggregates. Western blots developed with Tau-1 antibody (Binder et al., 1985) confirmed the up-regulation of dephosphorylation levels in Dp-AD O-tau after AP treatment (**Figure 4A**). Overexpression of HA-tau$_{151-391}$ in HeLa cells usually leads to aggregation in less than 10% of the transfected cells (HA positive) after 48 h transfection when examined by immunofluorescence (**Figure 4C**). Incubation with AD O-tau for 42 h significantly increased the proportion of aggregate-bearing cells (**Figures 4B,C**; Li et al., 2019; Gu et al., 2020). Unlike AD O-tau, Dp-AD O-tau did not promote the formation of tau aggregates (**Figures 4B,C**). In another set of experiments, 0.26 U AP was added into the culture medium of HA-tau$_{151-391}$-expressing cells together with AD O-tau and also inhibited AD O-tau-induced tau aggregation (**Figures 4B,C**). These results suggested that dephosphorylation of AD O-tau and/or its recruiting targets could help to reduce the formation of tau aggregates.

Next, HEK-293FT cells were transfected with HA-tau$_{151-391}$ and treated with AD O-tau or Dp-AD O-tau. The cell lysates were separated into RIPA-soluble and RIPA-insoluble fractions. Total and phosphorylated tau levels in each fraction were analyzed by Western blot (**Figure 5**). AD O-tau induced dramatic accumulation of total tau (**Figures 5A,B**) and tau phosphorylated at T181, T212, S214, and T217 (**Figures 5C,D**) in RIPA-insoluble fractions. However, compared with AD O-tau, Dp-AD O-tau treatment significantly decreased both total and phosphorylated tau deposit in RIPA-insoluble fractions (**Figure 5**). In both groups, the levels of RIPA-soluble tau were not grossly affected.

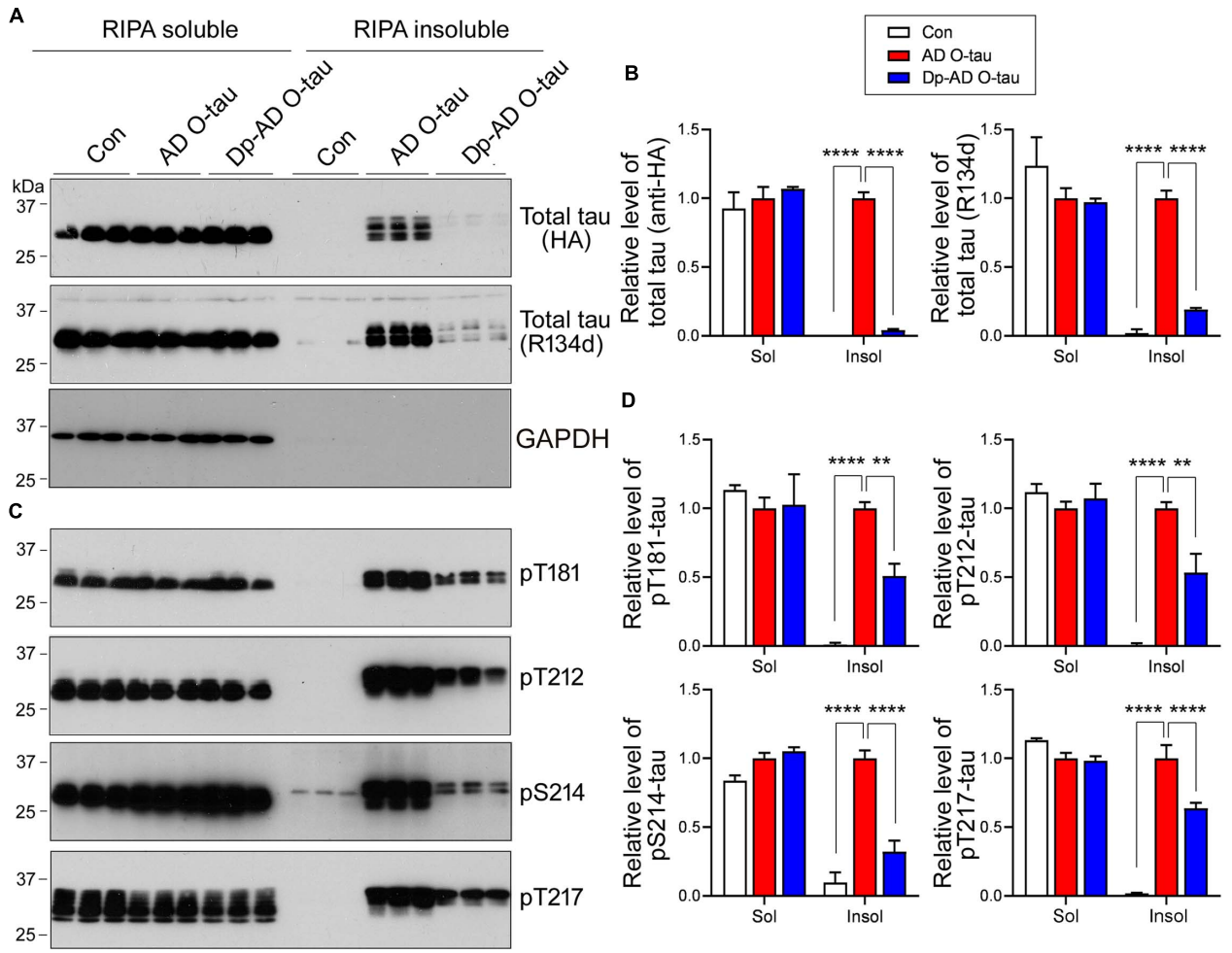


**FIGURE 5 |** Dephosphorylation of AD O-tau suppressed its ability to template tau aggregation. **(A–D)** HEK-293FT cells were transfected with pCI/HA-tau$_{151-391}$, treated with AD O-tau or Dp-AD O-tau and lysed with RIPA buffer. RIPA-soluble and -insoluble fractions were separated by centrifugation and analyzed with Western blots developed with antibodies toward HA, total tau (R134d), GAPDH **(A)**, or various phosphorylated tau **(C)**. The experiment was performed in triplicate. Relative levels of total **(B)** or phosphorylated **(D)** tau were measured. $^{**}P < 0.01$. $^{****}P < 0.0001$.

These data further supported that dephosphorylation of AD O-tau could suppress its ability in templating tau aggregation.

## DISCUSSION

Oligomeric tau derived from Alzheimer's brain is capable of capturing normal tau and templating misfolding and aggregation of tau protein and is therefore considered to display prion-like seeding properties. However, the characteristics of AD O-tau were not fully understood. Here, we reported that AD O-tau was mainly N-terminal truncated and C-terminal hyperphosphorylated. Dephosphorylation of AD O-tau significantly blocked its ability to capture tau and template tau aggregation.

NFTs composed of abnormally hyperphosphorylated tau are major pathological hallmarks of AD (Iqbal et al., 2016). Normal tau contains two to three phosphate groups. However, the phosphorylation levels of tau are increased by two to three times in AD brains. Hyperphosphorylation of tau alters the protein charge and conformation, which makes it easier to aggregate (Iqbal et al., 2016). Tau in AD brain displays in various pools—cytosolic and normal tau (AD-tau), cytosolic and hyperphosphorylated/oligomeric tau (AD P-tau), and PHF-tau (Kopke et al., 1993). AD P-tau, but not PHF tau, sequesters/captures normal tau *in vitro* to form filaments in a non-saturable manner (Alonso et al., 1994), which was the first identification of prion-like activity of AD P-tau. AD P-tau was isolated from the 27,000 to 200,000 × *g* fraction of AD brain homogenate by extraction in 8 M urea and was further purified by acid precipitation and ion chromatography (Kopke et al., 1993). It was found that 3,000 and 10,000 × *g* AD brain extracts, which presumably contained HMW proteins, showed significantly higher seeding activity than 150,000 × *g* extracts from which HMW tau was depleted by sedimentation (Takeda et al., 2015). The 3,000 and 10,000 × *g* extracts contain various

sizes of oligomeric tau (Takeda et al., 2015). Thus, AD O-tau in the fraction by sedimentation of AD brain homogenates from 27,000 to 235,000 × *g* predominantly varies in size of oligomeric tau, which is hyperphosphorylated and displays SDS- and β-mercaptoethanol-resistant HMW-tau. However, the size distribution of AD O-tau remains to be characterized.

Recently, studies utilizing high-resolution quantitative proteomics (Wesseling et al., 2020) and mass spectrometry (Dujardin et al., 2020) identified 26 post-translational modifications (PTM) in HMW-tau oligomers. Although tau PTM profiles were heterogeneous across subjects, the peptides spanning amino acid residues 195–209, 212–224, and 396–406 featured high-frequency phosphorylation and showed > 90% modification extent in AD patients (Wesseling et al., 2020). Phosphorylation on Ser262 was positively correlated with tau seeding capacity (Dujardin et al., 2020). Consistent with these studies, pT217, pSer262, and pS396/404 were dramatically elevated in AD O-tau compared to the control in this study. Ser422, which is not considered as a phosphorylation hotspot of HMW-tau oligomers (Wesseling et al., 2020), was also intensively hyperphosphorylated in AD O-tau (**Figure 1C**), reflecting heterogeneity in tau phosphorylation among individuals.

AD P-tau has litter activity to promote microtubule assembly and dephosphorylation with AP restored its activity (Alonso et al., 1994). AD P-tau associates with normal tau in solution forming large tangles and dephosphorylation abolishes its ability to aggregate with normal tau and prevents tangle formation (Alonso et al., 1996). Dephosphorylation of AD P-tau by PP2A inhibits its polymerization into PHF/straight filaments, and rephosphorylation of PP2A-dephosphorylated AD P-tau by kinases promotes AD P-tau assembly to PHF filaments (Wang et al., 2007). Intrahippocampal injection of AD P-tau (the same as AD O-tau mentioned in this work) induced tau pathology first at the injection sites, and then to the anatomically connected regions in mouse brain, mimicking the propagation of tau pathology observed in AD patients (Lasagna-Reeves et al., 2012a; Hu et al., 2016). Injection of dephosphorylated AD P-tau treated by protein phosphatase-2A dramatically diminished tau pathology, suggesting that dephosphorylation could restrict the seeding activity of AD P-tau (Hu et al., 2016). However, the mechanisms by which dephosphorylation inhibits the prion-like transmission of tau seeds remain unclear. Our results revealed that dephosphorylation of AD O-tau significantly reduced its ability to capture and template tau aggregation, which may explain why the prion-like seeding activity of dephosphorylated AD O-tau was limited *in vivo*.

AD O-tau and Dp-AD O-tau did not affect the levels of total or phosphorylated tau species in RIPA-soluble cell lysate. AD O-tau induced intensive accumulation of total and phosphorylated tau in the insoluble fraction, while dephosphorylation of AD O-tau significantly blocked that, suggesting that AD O-tau was prone to capture and template phosphorylated tau, and dephosphorylation could effectively inhibit its seeding activity. Therefore, phosphorylation of AD O-tau is crucial for the seeded aggregation of tau, and blockage of AD O-tau phosphorylation could be a potent way to diminish tau aggregation.

Inhibition of tau hyperphosphorylation has long been considered as a potential therapeutic approach for AD. A variety of therapy strategies targets tau hyperphosphorylation by interfering tau kinases or phosphatases (Iqbal et al., 2018). For example, the antidiabetic biguanide metformin induced activation of PP2A and reduced tau phosphorylation at PP2A-dependent epitopes in murine primary neurons and *in vivo* (Kickstein et al., 2010). Recently, a phase II clinical trial for metformin in treating amnestic mild cognitive impairment has been completed. In the present study, we showed that dephosphorylation of AD O-tau by AP, a phosphatase usually located on the outside surface of plasma membrane, significantly inhibited its prion-like seeding activity. AP directly added into the cell cultures could also reduce AD O-tau-induced aggregation of HA-tau$_{151-391}$ (**Figure 4**), showing a potential of inhibiting tau pathology. Actually, tissue non-specific alkaline phosphatase (TNAP) activity has been reported to increase in AD brain and plasma (Kellett and Hooper, 2015). Cell membrane-anchored TNAP is capable of dephosphorylating extracellular monomeric tau, which acts as an agonist of muscarinic M1 and M3 receptors, and provokes a sustained intracellular calcium increase leading to neuronal cell death (Diaz-Hernandez et al., 2010; Kellett and Hooper, 2015). Nevertheless, systemic administration of AP is still proposed as a potential therapeutic intervention against the pathology of AD, since sufficient anti-inflammatory AP in circulation might leave endogenous TNAP to perform its normal functions in the brain (Pike et al., 2015). Thus, the role of AP in modulating tau pathology *in vivo* is still worth further investigation.

In conclusion, dephosphorylation significantly decreased AD O-tau's activity in capturing tau and templating insoluble tau aggregates. Dephosphorylation of AD O-tau could be an effective way to inhibit its prion-like seeding activity and a potential target for the treatment of AD.

## DATA AVAILABILITY STATEMENT

The datasets presented in this article are not readily available because original western blots and immunostaining were used. Requests to access the datasets should be directed to DC, chudd@ntu.edu.cn and FL, fei.liu@opwdd.ny.gov.

## AUTHOR CONTRIBUTIONS

RW, LL, RS, YZ, NJ, and YT: performing experiments. DC and FL: designing the study, analyzing and interpreting the results, and drafting the manuscript. RW, LL, and FL: critical revision of the manuscript. All authors contributed to the article and approved the submitted version.

## FUNDING

This work was supported in part by funds from the Nantong University, New York State Office for People Developmental Disabilities, the Neural Regeneration Co-innovation Center of

Jiangsu Province and by grants from the U.S. Alzheimer's Association (DSAD-15-363172) and the Postgraduate Research and Practice Innovation Program of Jiangsu Province (KYCX18_2413).

## ACKNOWLEDGMENTS

We thank Dr. Peter Davies for contributing PHF-1 antibody and Dr. Lester I. Binder for providing Tau-1 antibody.

## REFERENCES

Alonso, A. C., Grundke-Iqbal, I., and Iqbal, K. (1996). Alzheimer's disease hyperphosphorylated tau sequesters normal tau into tangles of filaments and disassembles microtubules. *Nat. Med.* 2, 783–787. doi: 10.1038/nm0796-783

Alonso, A. C., Zaidi, T., Grundke-Iqbal, I., and Iqbal, K. (1994). Role of abnormally phosphorylated tau in the breakdown of microtubules in Alzheimer disease. *Proc. Natl. Acad. Sci. U. S. A.* 91, 5562–5566. doi: 10.1073/pnas.91.12.5562

Austin, T. O., Qiang, L., and Baas, P. W. (2017). "Chapter 4 – mechanisms of neuronal microtubule loss in Alzheimer's disease," in *Neuroprotection in Alzheimers Disease*, ed. I. Gozes (New York, NY: Sackler School of Medicine), 59–71. doi: 10.1016/b978-0-12-803690-7.00004-1

Binder, L. I., Frankfurter, A., and Rebhun, L. I. (1985). The distribution of tau in the mammalian central nervous system. *J. Cell Biol.* 101, 1371–1378. doi: 10.1083/jcb.101.4.1371

Boluda, S., Iba, M., Zhang, B., Raible, K. M., Lee, V. M., and Trojanowski, J. Q. (2015). Differential induction and spread of tau pathology in young PS19 tau transgenic mice following intracerebral injections of pathological tau from Alzheimer's disease or corticobasal degeneration brains. *Acta Neuropathol.* 129, 221–237. doi: 10.1007/s00401-014-1373-0

Braak, H., and Braak, E. (1991). Neuropathological stageing of Alzheimer-related changes. *Acta Neuropathol.* 82, 239–259. doi: 10.1007/bf00308809

Chu, D., and Liu, F. (2018). Pathological changes of Tau related to Alzheimer's disease. *ACS Chem. Neurosci.* 10, 931–944. doi: 10.1021/acschemneuro.8b00457

Clavaguera, F., Bolmont, T., Crowther, R. A., Abramowski, D., Frank, S., Probst, A., et al. (2009). Transmission and spreading of tauopathy in transgenic mouse brain. *Nat. Cell Biol.* 11, 909–913. doi: 10.1038/ncb1901

Diaz-Hernandez, M., Gomez-Ramos, A., Rubio, A., Gomez-Villafuertes, R., Naranjo, J. R., Miras-Portugal, M. T., et al. (2010). Tissue-nonspecific alkaline phosphatase promotes the neurotoxicity effect of extracellular tau. *J. Biol. Chem.* 285, 32539–32548. doi: 10.1074/jbc.m110.145003

Dujardin, S., Commins, C., Lathuiliere, A., Beerepoot, P., Fernandes, A. R., Kamath, T. V., et al. (2020). Tau molecular diversity contributes to clinical heterogeneity in Alzheimer's disease. *Nat. Med.* 26, 1256–1263.

Goedert, M., Jakes, R., Spillantini, M. G., Hasegawa, M., Smith, M. J., and Crowther, R. A. (1996). Assembly of microtubule-associated protein tau into Alzheimer-like filaments induced by sulphated glycosaminoglycans. *Nature* 383, 550–553. doi: 10.1038/383550a0

Grundke-Iqbal, I., Vorbrodt, A. W., Iqbal, K., Tung, Y. C., Wang, G. P., and Wisniewski, H. M. (1988). Microtubule-associated polypeptides tau are altered in Alzheimer paired helical filaments. *Brain Res.* 464, 43–52. doi: 10.1016/0169-328x(88)90017-4

Gu, J., Xu, W., Jin, N., Li, L., Zhou, Y., Chu, D., et al. (2020). Truncation of tau selectively facilitates its pathological activities. *J. Biol. Chem.* 295, 13812–13828. doi: 10.1074/jbc.ra120.012587

Hu, W., Zhang, X., Tung, Y. C., Xie, S., Liu, F., and Iqbal, K. (2016). Hyperphosphorylation determines both the spread and the morphology of tau pathology. *Alzheimers Dement.* 12, 1066–1077. doi: 10.1016/j.jalz.2016.01.014

Iqbal, K., Liu, F., and Gong, C. X. (2016). Tau and neurodegenerative disease: the story so far. *Nat. Rev. Neurol.* 12, 15–27. doi: 10.1038/nrneurol.2015.225

Iqbal, K., Liu, F., and Gong, C. X. (2018). Recent developments with tau-based drug discovery. *Expert. Opin. Drug Discov.* 13, 399–410. doi: 10.1080/17460441.2018.1445084

Kadavath, H., Hofele, R. V., Biernat, J., Kumar, S., Tepper, K., Urlaub, H., et al. (2015). Tau stabilizes microtubules by binding at the interface between tubulin heterodimers. *Proc. Natl. Acad. Sci. U. S. A.* 112, 7501–7506. doi: 10.1073/pnas.1504081112

Kellett, K. A., and Hooper, N. M. (2015). The role of tissue non-specific alkaline phosphatase (TNAP) in neurodegenerative diseases: Alzheimer's disease in the focus. *Subcell. Biochem.* 76, 363–374. doi: 10.1007/978-94-017-7197-9_17

Kickstein, E., Krauss, S., Thornhill, P., Rutschow, D., Zeller, R., Sharkey, J., et al. (2010). Biguanide metformin acts on tau phosphorylation via mTOR/protein phosphatase 2A (PP2A) signaling. *Proc. Natl. Acad. Sci. U. S. A.* 107, 21830–21835. doi: 10.1073/pnas.0912793107

Kopke, E., Tung, Y. C., Shaikh, S., Alonso, A. C., Iqbal, K., and Grundke-Iqbal, I. (1993). Microtubule-associated protein tau. Abnormal phosphorylation of a non-paired helical filament pool in Alzheimer disease. *J. Biol. Chem.* 268, 24374–24384. doi: 10.1016/s0021-9258(20)80536-5

Kremer, L., Dominguez, J. E., and Avila, J. (1988). Detection of tubulin-binding proteins by an overlay assay. *Anal. Biochem.* 175, 91–95. doi: 10.1016/0003-2697(88)90365-x

Lasagna-Reeves, C. A., Castillo-Carranza, D. L., Sengupta, U., Guerrero-Munoz, M. J., Kiritoshi, T., Neugebauer, V., et al. (2012a). Alzheimer brain-derived tau oligomers propagate pathology from endogenous tau. *Sci. Rep.* 2:700.

Lasagna-Reeves, C. A., Castillo-Carranza, D. L., Sengupta, U., Sarmiento, J., Troncoso, J., Jackson, G. R., et al. (2012b). Identification of oligomers at early stages of tau aggregation in Alzheimer's disease. *FASEB J.* 26, 1946–1959. doi: 10.1096/fj.11-199851

Li, L., Jiang, Y., Hu, W., Tung, Y. C., Dai, C., Chu, D., et al. (2019). Pathological alterations of Tau in Alzheimer's disease and 3xTg-AD mouse brains. *Mol. Neurobiol.* 56, 6168–6183. doi: 10.1007/s12035-019-1507-4

Miao, J., Shi, R., Li, L., Chen, F., Zhou, Y., Tung, Y. C., et al. (2019). Pathological Tau from Alzheimer's brain induces site-specific hyperphosphorylation and SDS- and reducing agent-resistant aggregation of Tau in vivo. *Front. Aging Neurosci.* 11:34. doi: 10.3389/fnagi.2019.00034

Mudher, A., Colin, M., Dujardin, S., Medina, M., Dewachter, I., Alavi Naini, S. M., et al. (2017). What is the evidence that tau pathology spreads through prion-like propagation? *Acta Neuropathol. Commun.* 5:99.

Pike, A. F., Kramer, N. I., Blaauboer, B. J., Seinen, W., and Brands, R. (2015). An alkaline phosphatase transport mechanism in the pathogenesis of Alzheimer's disease and neurodegeneration. *Chem. Biol. Interact.* 226, 30–39. doi: 10.1016/j.cbi.2014.12.006

Planel, E., Tatebayashi, Y., Miyasaka, T., Liu, L., Wang, L., Herman, M., et al. (2007). Insulin dysfunction induces in vivo tau hyperphosphorylation through distinct mechanisms. *J. Neurosci.* 27, 13635–13648. doi: 10.1523/jneurosci.3949-07.2007

Takeda, S., Wegmann, S., Cho, H., DeVos, S. L., Commins, C., Roe, A. D., et al. (2015). Neuronal uptake and propagation of a rare phosphorylated high-molecular-weight tau derived from Alzheimer's disease brain. *Nat. Commun.* 6:8490.

Tatebayashi, Y., Iqbal, K., and Grundke-Iqbal, I. (1999). Dynamic regulation of expression and phosphorylation of tau by fibroblast growth factor-2 in neural progenitor cells from adult rat hippocampus. *J. Neurosci.* 19, 5245–5254. doi: 10.1523/jneurosci.19-13-05245.1999

von Bergen, M., Barghorn, S., Biernat, J., Mandelkow, E. M., and Mandelkow, E. (2005). Tau aggregation is driven by a transition from random coil to beta sheet structure. *Biochim. Biophys. Acta* 1739, 158–166. doi: 10.1016/j.bbadis.2004.09.010

Wang, J. Z., Grundke-Iqbal, I., and Iqbal, K. (1996). Restoration of biological activity of Alzheimer abnormally phosphorylated tau by dephosphorylation with protein phosphatase-2A, -2B and -1. *Brain Res. Mol. Brain Res.* 38, 200–208. doi: 10.1016/0169-328x(95)00316-k

Wang, J. Z., Grundke-Iqbal, I., and Iqbal, K. (2007). Kinases and phosphatases and tau sites involved in Alzheimer neurofibrillary degeneration. *Eur. J. Neurosci.* 25, 59–68. doi: 10.1111/j.1460-9568.2006.05226.x

Wang, Y., Garg, S., Mandelkow, E. M., and Mandelkow, E. (2010). Proteolytic processing of tau. *Biochem. Soc. Trans.* 38, 955–961. doi: 10.1042/bst0380955

Weingarten, M. D., Lockwood, A. H., Hwo, S. Y., and Kirschner, M. W. (1975). A protein factor essential for microtubule assembly. *Proc. Natl. Acad. Sci. U. S. A.* 72, 1858–1862. doi: 10.1073/pnas.72.5.1858

Wesseling, H., Mair, W., Kumar, M., Schlaffner, C. N., Tang, S., Beerepoot, P., et al. (2020). Tau PTM profiles identify patient heterogeneity and stages of Alzheimer's disease. *Cell* 183:e13.

Wischik, C. M., Schelter, B. O., Wischik, D. J., Storey, J. M. D., and Harrington, C. R. (2018). Modeling prion-like processing of Tau protein in Alzheimer's disease for pharmaceutical development. *J. Alzheimers Dis.* 62, 1287–1303. doi: 10.3233/jad-170727

Zhang, Z., Song, M., Liu, X., Kang, S. S., Kwon, I. S., Duong, D. M., et al. (2014). Cleavage of tau by asparagine endopeptidase mediates the neurofibrillary pathology in Alzheimer's disease. *Nat. Med.* 20, 1254–1262. doi: 10.1038/nm.3700

Zhou, Y., Shi, J., Chu, D., Hu, W., Guan, Z., Gong, C. X., et al. (2018). Relevance of phosphorylation and truncation of Tau to the etiopathogenesis of Alzheimer's disease. *Front. Aging Neurosci.* 10:27. doi: 10.3389/fnagi.2018.00027

**Conflict of Interest:** The authors declare that the research was conducted in the absence of any commercial or financial relationships that could be construed as a potential conflict of interest.